Nanotechnology

Porous SnO_2-Cu_xO nanocomposite thin film on carbon nanotubes as electrodes for high performance supercapacitors

To cite this article before publication: Farhad Daneshvar *et al* 2018 *Nanotechnology* in press https://doi.org/10.1088/1361-6528/aae5c6

Porous SnO_2-Cu_xO nanocomposite thin film on carbon nanotubes as electrodes for high performance supercapacitors

Farhad Daneshvar [a], *Atif Aziz* [b]*, *Amr M. Abdelkader* [c], *Tan Zhang* [a], *Hung-Jue Sue* [a]*, *and Mark E. Welland* [b]

[a.] Polymer Technology Centre, Department of Materials Science and Engineering, Texas A&M University, College Station, TX 77843, USA.

[b.] Nanoscience Centre, Department of Engineering, University of Cambridge, CB3 0FF, UK.

[c.] Faculty of Science and Technology, Bournemouth University, Poole House, Talbot Campus, Poole, Dorset BH12 5BB

KEYWORDS: pseudo-capacitance, carbon nanotube, copper oxide, electroless deposition, supercapacitor

ABSTRACT: Metal oxides are promising materials for supercapacitors due to their high theoretical capacitance. However, their poor electrical conductivity is a major challenge.

* Corresponding authors: A. Aziz: aa267@cam.ac.uk, H.J. Sue: hjsue@tamu.edu

Hybridization with conductive nanostructured carbon-based materials such as carbon nanotubes (CNTs) has been proposed to improve the conductivity and increase the surface area. In this work, CNTs are used as template for synthesizing porous thin films of SnO_2-CuO-Cu_2O (SnO_2-Cu_xO) via electroless deposition (ED) technique. Tin with its high wettability and electrical conductivity acts as an intermediate layer between copper and CNTs and provides a strong interaction between them. We also observed that by controlling the interfacial characteristics of CNTs and varying the composition of the electroless bath, the SnO_2-Cu_xO thin film morphology can be easily manipulated. Electrochemical characterizations show that CNT/SnO_2-Cu_xO nanocomposite possesses pseudocapacitive behavior that reaches a specific capacitance of 662 F/g and the retention is 94% after 5000 cycles which outperforms any known copper and tin-based supercapacitors in the literature. This excellent performance is mainly attributed to high specific surface area, small particle size, synergistic effect of Sn, and conductivity improvement by using CNTs. The combination of CNTs and metal oxides holds promise for supercapacitors with improved performance.

1. INTRODUCTION

Stringent environmental regulations, ever-increasing interest in electric vehicles (EV), and their fast market growth have enticed automotive companies to push for EVs sooner than anticipated. Extensive work on rechargeable batteries made this transition feasible. However, there are still significant obstacles to overcome. One of the deficiencies of rechargeable batteries occurs during acceleration of EVs when the battery is required to provide a huge amount of energy in a short period of time. This rapid energy depletion can damage the electrode materials, and reduce the battery's lifetime [1]. Therefore, there has been an effort to develop novel electrode materials with

higher power density and better stability [2-3]. An alternative solution has been implemented: a complementary system alongside the battery, which has high cyclability and ability to provide the demanded energy during acceleration [4-5]. Supercapacitors or electrochemical capacitors (ECs) are an attractive option due to their high power density, long life span, high cyclic efficiency, safety and rapid charge-discharge rates [5-7].

Based on energy storage mechanisms, supercapacitors are categorized into two groups: electrical double layer capacitors and pseudocapacitor. The former purely works based on electron storage at double layer while in the latter, faradic redox reactions occur which results in significantly higher specific capacitance and energy density [8-9]. Pseudocapacitors typically are made of either polymers or transition metal oxides (TMOs). While polymers have good specific capacity and electrical conductivity, they suffer from poor cyclability due to substantial volume changes [10]. TMOs, on the other hand, generally possess higher specific capacitance, but their electrical conductivity is poor [11-12]. Because pseudocapacitance relies on faradic reactions at the surface, a higher specific surface area provides more sites for metal oxide redox reactions, which improves the specific capacitance of the TMOs. In addition to specific surface area, electrical conductivity and microstructure also play major roles on capacitive behavior of TMOs.

Copper oxide is one of the promising TMOs for supercapacitor applications. It is an inexpensive and abundant material that possesses high theoretical capacity [13-15]. Therefore, recently these oxides, either in CuO or Cu_2O form, have attracted considerable interest as EC electrode material [14-20]. However, the electrochemical performance of these oxides suffers due to low conductivity and limited specific surface area [20-21]. To tackle the obstacle of low electrical conductivity, hybridization with conductive carbon-based materials such as carbon black, graphene, or carbon nanotubes (CNTs) has been suggested [17, 22-26]. Among these, CNTs have attracted particular

attention due to their high electrical conductivity, specific surface area, mechanical strength, electrochemical stability, and low electrical percolation threshold. As Liu et al. [18] has shown, by introducing CNTs to electrode materials a conductive network is created which facilitates charge transfer through the electrode and enhances the specific capacitance of CuO nano-sheets significantly.

However, progress in integrating CNTs in supercapacitors has been limited. For instance Zhang et al. [23] observed that substituting CNT for carbon black as an additive in CuO electrode material not significantly increased the specific capacitance (from 137 F/g to 150 F/g). Nevertheless, previous research has shown that using CNTs during the synthesis of active material can yield advantages far beyond just forming a conductive network. In this case, CNTs can yield strong bonds with metal oxides by acting as supports or templates for nucleation and growth of active material. This not only enhances the charge transfer, but also results in size refinement, hinders agglomeration, and creates a coarse and mesoporous structure that results in higher capacitance through easier charge transfer and higher specific surface area [25, 27-29].

In addition to hybridization with carbon nanostructures, hybridization with transition metal oxides has shown to be a promising method for improving the electrochemical performance of electrodes in supercapacitors [29-32]. For instance, Sugimoto et al. [31] reported that by introducing VO_2 to RuO_2 the specific surface area was tripled and specific capacitance reached to 1210 F/g, which exceeds that of Ru_2O electrode by 60%. In addition to increasing the surface area, doping a secondary oxide can improve the electrochemical performance by enhancing the conductivity, uniformly dispersing the active material or refining the particle size. Stannic oxide is one of the oxides that has been studied as an additive in composite electrodes. SnO_2 not only has the conventional redox properties, but also is inexpensive, has high wettability, and relative to other

TMOs, has higher electronic conductivity [5]. It has been observed that adding SnO_2 has a synergistic effect on electrode performance especially through increasing electrical conductivity and facilitating electron and proton conduction [32]. Therefore, regardless of the material type, by choosing a suitable additive the electrochemical performance of the electrode can be enhanced.

In this work multi-walled CNTs (MWCNTs) were used as a template for growth of tin and copper oxides (CuO_x-SnO_2) nanoparticles using electroless deposition (ED). ED is a simple and scalable technique which provides morphology control by easily changing the parameters, such as pH and bath composition, and can produce rough and porous structures [33-34]. Moreover, by using MWCNTs we were able to engineer the morphology of SnO_2-Cu_xO thin film in nanoscale and create a one-dimensional (1D) porous structure which offers high surface area and short transport/diffusion pathways for electrons/ions which leads to fast kinetics and high capacity. Strong bonding between the thin film and MWCNTs and 1D porous SnO_2-Cu_xO structure provides an excellent cycle stability through accommodating the volume changes caused by faradic reactions. Electrochemical tests have shown that deposition of tin and copper oxides on CNTs can result in a hybrid material which outperforms any reported copper-based and tin-based supercapacitors in the literature with respect to specific capacitance and cyclability (Table S1).

2. EXPERIMENTAL PROCEDURE

2.1. Materials and methods

Multiwall carbon nanotubes (MWCNT) with a purity of 95 wt.%, diameter of 20-40 nm and length of 10-30 μm were supplied by Arkema Inc. All other chemicals were obtained from Sigma-Aldrich and were used as received. For obtaining a good dispersion they were exfoliated according to previous report [35]. Briefly, 250 mg as-received MWCNTs were added to a mixture

of H_2SO_4 (45 mL) and HNO_3 (15 mL) at a 3:1 volume ratio. This mixture was sonicated in a sonication bath for two hours at 25 °C [36] and then washed with DI water.

Synthesis of SnO_2-Cu_xO/CNT hybrid structure by ED consists of several steps which are schematically represented in Figure 1. First 50 mg of oxidized MWCNTs were added to a 50 ml aqueous solution of $SnCl_2$ (0.98 g) and 0.1 ml HCl (37 wt.%). The mixture was sonicated for 15 minutes, and then washed with DI water. CNTs usually have weak interactions with metallic particles. In supercapacitor applications this can result in lower conductivity and detachment of metal oxides from the CNTs. Tin has a high wetting capability and therefore readily attaches to the surface of MWCNTs. Tin layer will act as an intermediate layer for adsorption of other metallic-based particles during following processing steps. In the next step, sensitized MWCNTs are added to 50 ml DI water solution containing 0.007 g $PdCl_2$ and 0.1 ml HCl (37 wt.%) and sonicated for 15 minutes. During this stage (i.e. activation), palladium ions replace a portion of the tin particles on the surface of MWCNTs and act as catalysts for nucleation and growth of copper. Finally after washing with DI water, activated MWCNTs are dispersed in 50 ml copper electroless deposition (ED) bath with the chemical composition presented in Table 1. After 15 minutes of stirring at 60 °C, 0.2 ml formaldehyde solution was added gradually to reduce the copper ions. After 30 minutes of stirring at 60 °C copper coated MWCNTs were washed and separated by centrifuge.

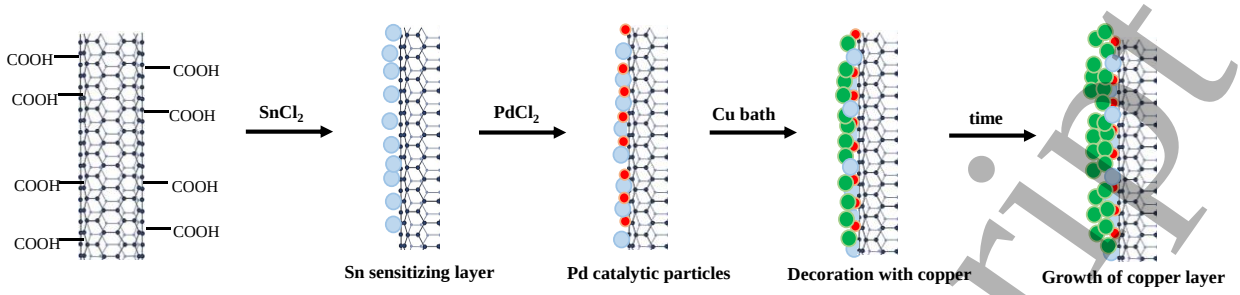

Figure 1. A schematic of an electroless deposition process on CNTs. Blue, red and green spheres represent Sn, Pd and Cu particles respectively.

2.2. Characterization

For assessing the coating morphology transmission electron microscope (TEM, FEI Teccai G2 S-Twin, Philips) was used. The crystallographic phases of all of the samples were investigated using an X-ray diffractometer (XRD, Bruker D8 Advance ECO) with CuK_{α} incident radiation (λ=0.1506 nm). X-ray photoelectron spectroscopy (XPS) was obtained from an Omicron's DAR 40 dual Mg/Al X-ray source for XPS measurements and the HIS 13 He UV source for UPS measurements. STEM and EDX images were obtained using a FEI Tecnai Osiris S/TEM working at 200 keV. The EDX detectors are FEIs Super-X system employing 4 Bruker silicon drift detectors (SDD) for high collection efficiency (>0.9 sr solid angle) and high count rates (>250 kcps).

2.3. Electrochemical Tests

The electrochemical performance of the supercapacitors were tested in a conventional three-electrodes (versus Ag/AgCl)) and two electrodes coin cells. All the electrochemical measurements including cyclic voltammetry and galvanostatic charge/discharge were conducted using Iviumstat Electrochemical Interface. Cyclic voltammetry tests have been carried out with the two-electrode cells. Electrodes were prepared by mixing the hybrid material with poly-vinylidene fluoride (PVDF) and carbon black (CB) (80:10:10 in mass ratio) using a pestle and

mortar. Cyclic voltammetry (CV) measurements were recorded in a 6 M KOH aqueous electrolyte in the range of -0.4 to 0.4 V at different scan rates.

Table 1. Chemical composition of copper electroless bath.

Chemical composition	Quantity
$CuSO_4.5H_2O$	6.2 g/l
2Na-EDTA	40 g/l
Na_2SO_4	35 g/l
HCOONa	60 g/l
CHOH (37 vol% in water)	20 ml/l
Temperature	60 °C
pH (NaOH)	13

3. RESULTS AND DISCUSSION

The chemical composition of the hybrid system was investigated by XPS, XRD and EDX. Figure 2a represents the XPS spectrum where the peaks at binding energies of 284.4, 486.5 and 933.9 eV correspond to C 1s, Sn 3d and Cu 2p, respectively. The C 1s peak is associated with the sp^2 C-C bond of MWCNTs and can be deconvoluted into C=C at 284.3 eV, C-O at 285.8 eV and C=O at 288.2 eV [37-39]. The presence of these peaks underneath the C 1s is an indication of functional groups on the surface of MWCNTs created during acid treatment. These groups not only enhance the bonding between the metal oxides and MWCNTs, but also increase the wettability and hydrophilicity of the hybrid system which helps increase electrolyte ion transport within the structure. Moreover, Pan, et al. [40] observed redox peaks in CV curves of functionalized CNTs indicating that these oxygenated groups on the surface may induce faradic redox reactions which can enhance the specific capacitance. Finally, it should be noted that proper acid treatment can increase the specific surface area of MWCNTs either by creating defects at the surface or

dissolving the catalysts and opening the tube ends. As a result, due to capillary forces during ED process, metallic ions can diffuse and deposit inside the tube.

The peaks related to Sn are situated at 495 eV and 486.6 eV belonging to Sn 3d3/2 and Sn 3d5/2, respectively. These results are identical to the reference data for Sn 3d in SnO_2 [41]. As represented in Figure 2d, the high-resolution XPS spectra for Cu consist of 4 peaks. The peaks observed at 933.9 eV and 953.3 eV are attributed to Cu 2p3/2 and Cu 2p1/2, respectively [42]. Moreover, two strong satellite peaks are seen at higher binding energies compared to the main peaks: a sharp peak at 962.35 eV and a broad peak between 941 to 945 eV. The overall spectrum is similar to CuO. However, by analyzing the main Cu 2p1/2 peak more carefully, it can be noted that at lower binding energies another peak exists; therefore, the Cu 2p3/2 peak can also be deconvoluted into two peaks by Gaussian method. The new peak at lower binding energy (932.3 eV) has a low intensity and is characteristic of Cu_2O [43-44], confirming that CuO and Cu_2O oxides coexist in the deposited coating which is in accordance with XRD results (Figure 2e).

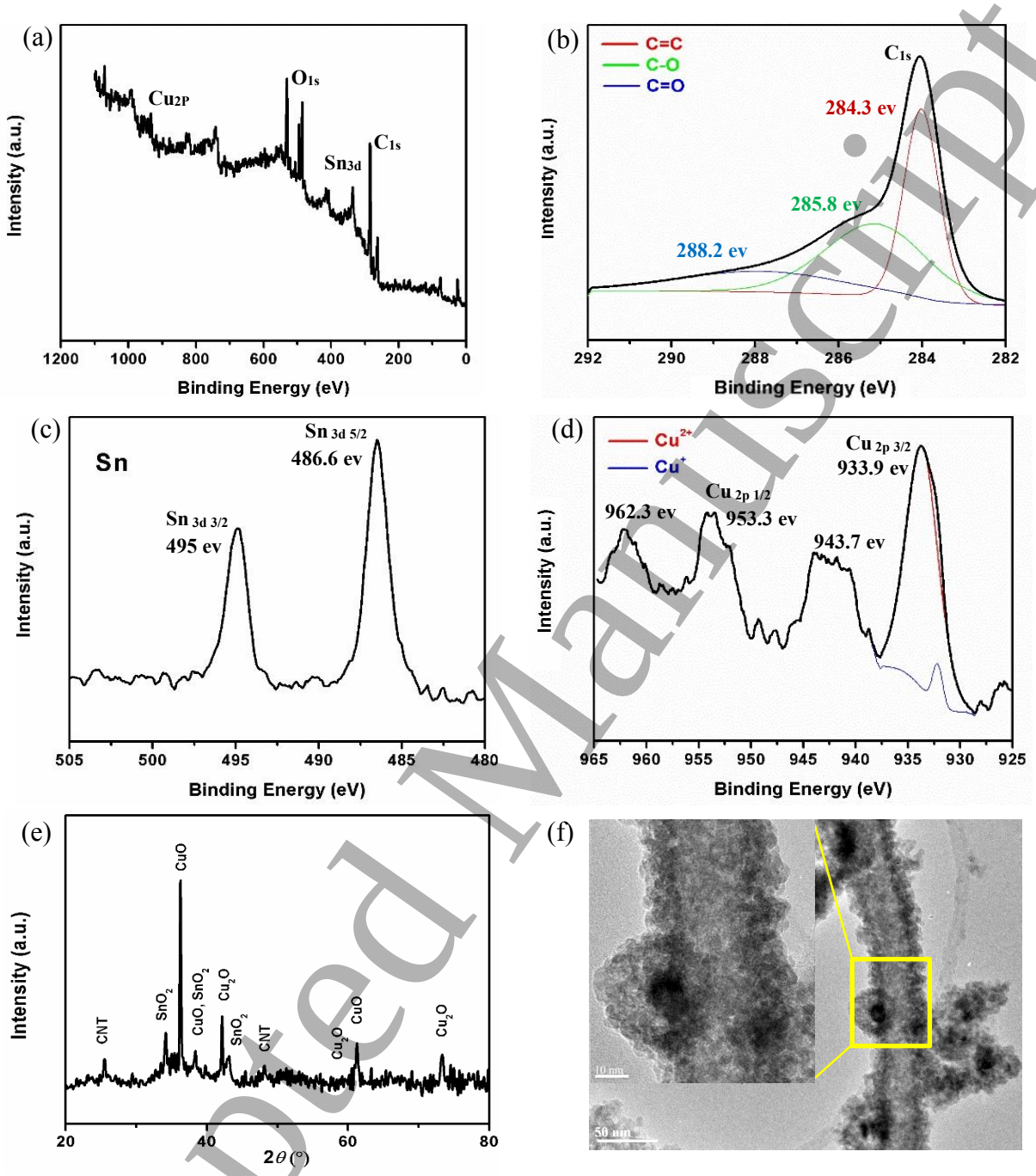

Figure 2. XPS spectra of (a) hybrid system, (b) C 1s of CNT, (c) Sn 3d of SnO_2, (d) Cu 2p spectrum of CuO/Cu_2O, (e) XRD of the hybrid sample and (f) TEM images of coated CNTs. The scale bar in the intersected picture is 10 nm.

The morphology and microstructure of the hybrid system is represented in Figure 2f. It can be observed that the coating has a rough surface in nanoscale and contains pores less than 1 nm in size which makes this structure suitable for aqueous electrolytes [6]. Also, thickness of the coating

is generally 10-15 nm. Such a fine and porous structure provides a large accessible surface area and facilitates electrolyte penetration [2]. As a result most of the nanocomposite can take part in faradic reactions which has a positive effect on capacitance.

From STEM images and nanoscale elemental maps (Figure 3) of the electroless deposited MWCNT, it is observed that the tube is present at the core and is uniformly covered with tin and copper oxides. Images with lower magnification (Figure S2) show that some of the MWCNTs are completely and some partially covered with metal oxide layer (the effect of coating density will be discussed). No observable x-ray signal was seen from palladium, which could be due the fact that it was completely covered by the Cu layer and the quantity was too small to be detectable.

As can be observed in Figures 2f and 3, MWCNTs act as a template for deposition of fine copper nanoparticles and created a core-shell structure [45]. The C-OH and C=O bonds created during the acid treatment provide sites for adsorption of Sn/palladium ions. Since these defects eventually act as nucleation sites for copper, it is expected that application of functionalized MWCNTs also plays a major role in size refinement and morphology control [28]. The adsorbed Pd/Sn nuclei subsequently act as catalyst for reduction and nucleation of copper according to the following reaction [46]:

$$2HCHO + Cu^{2+} + 4OH^{-} \rightarrow 2HCOO^{-} + H_2 + 2H_2O + Cu \quad (1)$$

It should be noted that the produced copper in particles are in nanoscale therefore dissolved oxygen in water readily oxidizes the Cu and Sn particles. This can lead to finer particle size since copper growth favorably occurs on the fresh copper nuclei and oxidation hinders copper particle growth.

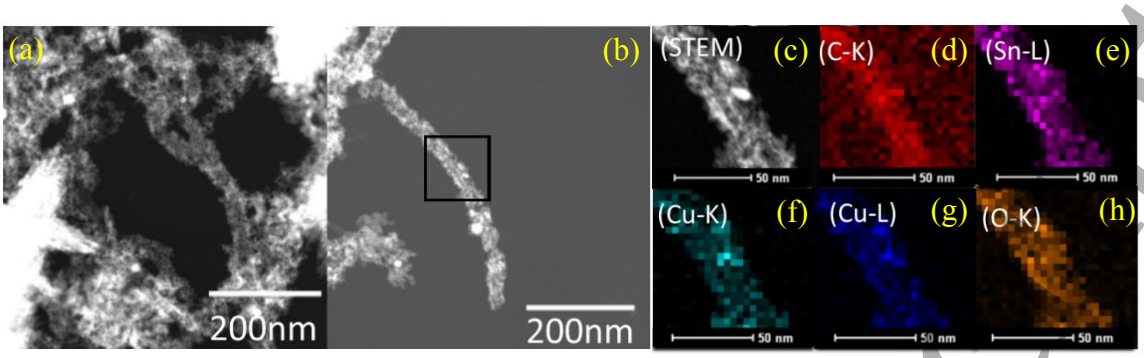

Figure 3. STEM (a-c) and EDX (d-h) of an electroless coated representative CNT. Black box shows the location where the elemental map is obtained.

Using a MWCNT backbone structure not only improves the electrical conductivity but also increases the surface area. As it can be seen in Figure 2f, deposited metal oxides adopt the 1-D structure of MWCNT and the maximum thickness reaches to 15 nm. By considering the porous structure of the thin film, we can assume that most of metal oxides are accessible by the electrolyte. Moreover, assembling these 1-D hybrid structures of SnO_2-Cu_xO/CNT creates a three-dimensional (3-D) porous conductive network which further enhances the electrolyte accessibility and promotes both electron and ion transport within the electrode material. Furthermore, we observed that the morphology, density and size of deposited particles are affected by the MWCNT surface modification method. If the oxidation of CNTs is not sufficient, the coating will be scarce (as shown in the supplementary information S1) It should be noted that if the MWCNTs are fully coated with a thick layer of metal oxide, the conductivity of the hybrid system and as a result the capacitance of the electrode reduces [47]. It should be added that before performing TEM analysis, the sample was diluted in water and went through a sonication step. The fact that the coating is still attached after the sonication process shows that there is a strong interaction between the MWCNT and copper coating which can help to preserve the integrity of the electrode through charge-discharge cycles and enhance the capacitance performance of the hybrid material [47-49].

The electrochemical performance of the supercapacitor electrode was assessed by cyclic voltammetry (CV) and galvanostatic charge/discharge tests in a two-electrode coin cell configuration. Figure 4a shows the CV curves of the MWCNT and the SnO_2-Cu_xO/CNT electrodes at scan rates 5 mV/s using a potential window from -0.4V to 0.4 in 6 M KOH solution. The CV curves of pure MWCNT show a nearly rectangular shape without any obvious redox peaks, indicating that the capacitance is primarily originated from double-layer capacitance. By utilizing SnO_2-Cu_xO/CNT as the electrode, two distinct reduction peaks and one oxidation peak were observed. While the observation of the redox peaks is a sign of pseudocapacitance contribution. The background current is significantly higher for SnO_2-Cu_xO/CNT than for MWCNT, which couples with the rectangular shape of the CV curve, suggests a double layer capacitance contribution from the copper oxide coating on MWCNTs. The pseudocapacitance behavior in the CV scans is associated with the following reactions [14, 50-51]:

$$CuO + H_2O + 2e^- \rightarrow Cu_2O + 2OH^- \quad (2)$$

$$Cu_2O + H_2O + 2OH^- \rightarrow 2Cu(OH)_2 + 2e^- \quad (3)$$

$$CuOH + OH^- \rightarrow Cu(OH)_2 + e^- \quad (4)$$

$$CuOH + OH^- \rightarrow CuO + H_2O + e^- \quad (5)$$

$$SnO_2 + H_2O + e^- \rightarrow SnOOH + OH^- \quad (6)$$

$$SnOOH + e^- \rightarrow SnO + OH^- \quad (7)$$

One anodic peak and two cathodic peaks are observed in the operated potential range. The anodic peak can be ascribed to the oxidation of either Cu_2O or CuOH to CuO and/or $Cu(OH)_2$. It is possible that these two peaks have overlapped with each other. The cathodic peaks are attributed to the reduction of CuO and/or $Cu(OH)_2$ to Cu_2O and/or CuOH [14, 50]. It should be

noted that based on the previous works in this potential range SnO_2 does not show clear redox peaks [51-55] therefore it can be concluded that the overall shape of the CV curve is dominated by copper oxides performance. Also it has been reported before that the pseudocapacitance contribution of CuO is mainly governed by the reduction of Cu^{2+} to Cu^{+} in KOH solutions [3, 56-57]. Detecting two reduction peaks in the current study suggests that copper ions are existing in two oxidation states which is in agreement with XPS results. It is possible that the presence of carbon stabilizes the Cu^{+} oxidation states. At early stages of ED process it was observed that if the tube ends are open due to capillary forces tin and copper deposit inside the MWCNTs (Figure S4). These well-defined and narrow channels inside CNTs possess unique electronic properties that make the confined metal oxide particles stay in a more reduced state. This phenomenon has been previously reported for some metal oxides such as manganese [58], tin [59], and Iron [60]. This confinement can enhance the capacitance of the nanocomposite electrode; due to curvature, π-electron is denser at the outer surface of CNT which leads to electron deficiency inside interior hollow cavity of CNTs. As a result the charge transfers from electron donor metal oxide to compensate for the electron deficiency inside the nanotube. This is helpful in adsorption-desorption process of positive ions in the electrolyte such as K^{+} and H^{+} [58-59] and enhance the capacity. Also density functional theory calculations of Ng et al. [61] and experimental works on confined Sn particles within CNTs [59] have shown that CNTs with encapsulated Sn has higher electrical conductivity compared with standalone CNTs which also can enhance the capacitance.

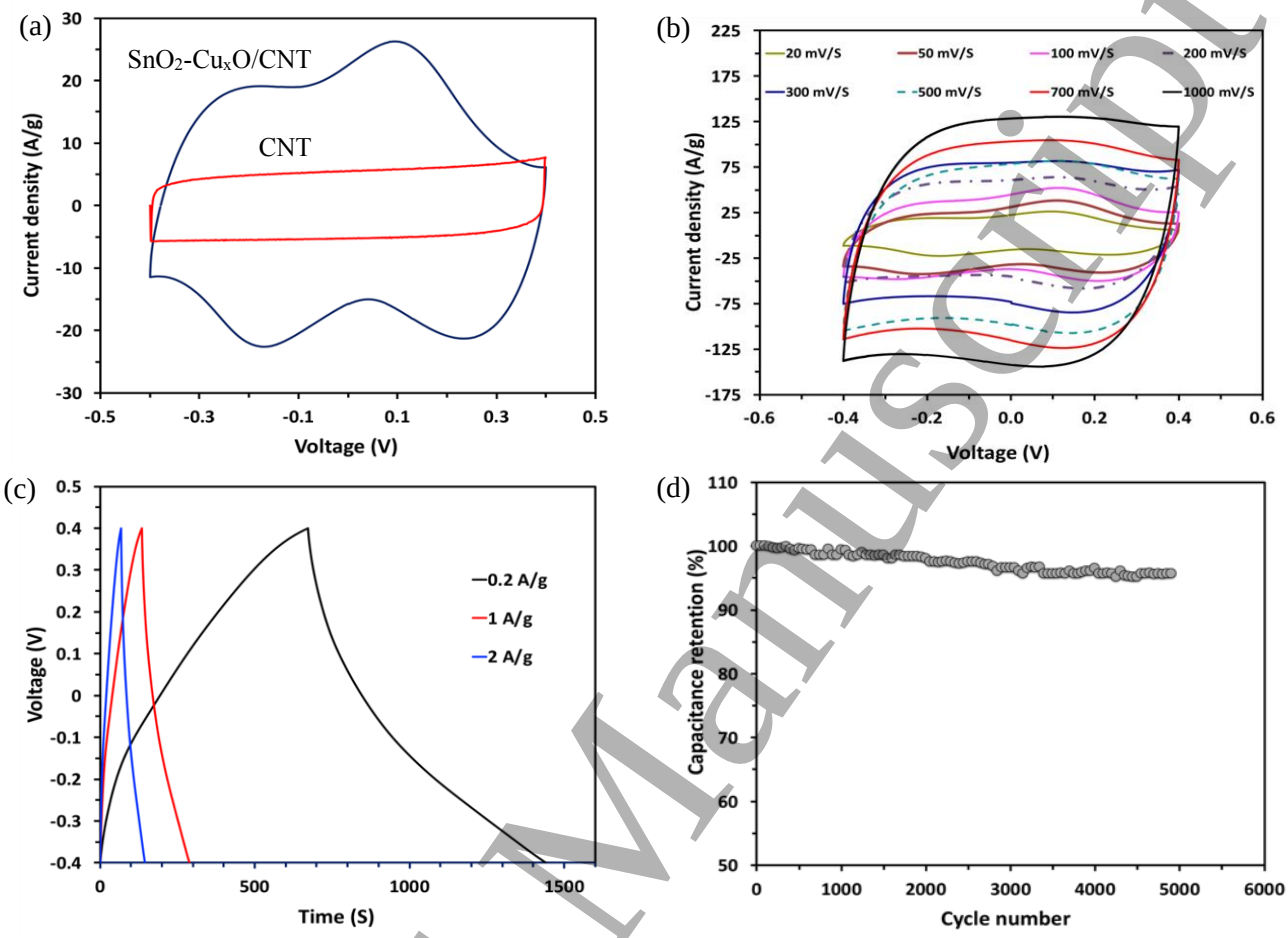

Figure 4. The electrochemical performance of the SnO_2-Cu_xO/CNT electrode (a) CV of CNT and electroplated CNT electrode at 5 mV/S, (b) CV of the electroplated electrode at different scan rate (c) charge discharge curve at different current density, and (d) Cycling performance at current density of 1 A g^{-1}.

The capacitance performance of the core-shell structure was evaluated with cyclic voltammograms in a scan rate range of 20 to 1000 mV/s. As it can be observed in Figure 4b, with increasing scan rate, the redox peaks almost vanished, and the CV curves of the hybrid system become featureless, suggesting the faradic reactions are diffusion limited. The CV curve, however, maintains a nearly rectangular and good mirror images of the zero-current line even at high scan rates indicating an ideal capacitive behavior [19].

We have also used galvanostatic charge/discharge analysis for practical evaluation of the SnO_2-Cu_xO/CNT electrode capacitance in an alkali electrolyte (Figure 4c). The curve for the MWCNT

is nearly triangular and shows linear charge and discharge profiles, indicating purely capacitive behavior [62]. The SnO_2-Cu_xO/CNT shows a pair of bending points at potentials close to those in the CV curve. In both cases, the charge/discharge curves were symmetrical, indicating good electrochemical capacitive characteristics and excellent reversible redox reaction. Interestingly, the SnO_2-Cu_xO/CNT electrode displays almost no drop in internal resistance (IR) at the beginning of the discharge curve, indicating low overall IR of the nanocomposite electrode. The corresponding specific capacitance was calculated from the slopes of the discharge branch of the curve using the following equation:

$$C_s = \frac{4\,i}{-\frac{\Delta V}{\Delta t}m} = \frac{4\,i}{-slope \times m} \quad (1)$$

In which i is the current applied, $\Delta V/\Delta t$ is the slope of the discharge curve, and m is the mass of the nanocomposite electrode. The SnO_2-Cu_xO/CNT electrode can reach a specific capacitance as high as 662 F/g at 0.2 A/g. To our knowledge, this value is the highest reported in the literature for CuO based capacitor (about 569 F/g and 545 F/g for binder free CuO nano-sheets on Ni foam at similar scan rates) [15, 63]. The supercapacitor electrode was cycled for 5000 cycles and retained about 94% of its initial capacitance (Figure 4d) which is much superior compared to previous results [15, 63]. The excellent cyclability performance is attributed to the 1D porous structure and strong bonding between the constituents of the nanocomposite. 1D porous structure provides space for accommodating the volume changes during charge-discharge cycles. Strong bonding between the metal oxides and MWCNTs helps to preserve the integrity of the electrode material. In this regard tin's role is very crucial. It has relatively high electrical conductivity and excellent wettability. It readily adheres to the MWCNTs surface and makes it suitable for nucleation and growth of copper particles. Because copper is directly nucleated on tin, a strong interaction between these two components exists. Therefore tin oxide acts as an intermediate layer between

copper oxide and the MWCNTs. In addition, using tin oxide can have other synergistic advantages, i.e. particle size refinement and enhancement of electronic and redox properties of the electrode material [32, 64].

To summarize, the improved performance of the SnO_2-Cu_xO/CNT electrode can be attributed to the following aspects. (i) abundant void space between the porous nanostructures not only provide short distance for the diffusion of the electrolyte but also offer a large number of electroactive sites for faradaic redox reactions to take place, hence improving the pseudo-capacitive performance, (ii) the 3D carbon network works as the backbone that provides mechanical integrity and facilitates electronic transportation within the electrodes (iii) SnO_2 has a synergistic effect on Cu_xO performance through wetting the surface of MWCNTs, modifying the particle size and enhancing the conductivity of the nanocomposite, (iv) by acid treatment the ends of MWCNTs open which results in infiltration and capsulation of metal oxide particles inside the MWCNT. These confined particles possess higher conductivity, smaller particle size and can facilitate diffusion of ions in the electrolyte which leads to higher capacitance, and (v) anchoring the CuO_x nanoparticles, which minimizes aggregation and maximizes high specific surface area.

4. CONCLUSION

Three-dimensional network of SnO_2-Cu_xO/CNT wire structure with MWCNTs as the substrate and copper oxide as the coating were synthesized through an electroless deposition technique. This facile and controllable processing method produces a unique core-shell structure with high porosity which enables fast ion and electron transports. The copper oxide nanoparticles enhance the capacitance through additional faradic redox reactions. The new hybrid shows excellent electrochemical performance as a supercapacitor electrode with a specific capacity of 662 F/g.

The electrode is robust and capable of retaining more than 94% of its original capacity after 5000 cycles, indicating excellent electrochemical stability. Such an outstanding performance suggests that by engineering the CNTs surfaces and utilizing ED method, high capacity energy storage materials can be produced. Moreover, this method can be easily applied to other metal oxides to produce high performance supercapacitor electrodes.

CONFLICT OF INTEREST

There are no conflicts to declare.

ACKNOWLEGMENTS

All the authors acknowledge the support of the Lloyd's Register Foundation, London, UK, who has funded this research through their grants to protect life and property by supporting engineering-related education, public engagement and the application of research.

REFERENCES

1. Peterson, S. B.; Apt, J.; Whitacre, J., Lithium-ion battery cell degradation resulting from realistic vehicle and vehicle-to-grid utilization. *Journal of Power Sources* **2010,** *195* (8), 2385-2392.
2. Simon, P.; Gogotsi, Y., Materials for electrochemical capacitors. *Nature materials* **2008,** *7* (11), 845.
3. Ameri, B.; Davarani, S. S. H.; Roshani, R.; Moazami, H. R.; Tadjarodi, A., A flexible mechanochemical route for the synthesis of copper oxide nanorods/nanoparticles/nanowires for supercapacitor applications: The effect of morphology on the charge storage ability. *Journal of Alloys and Compounds* **2017,** *695*, 114-123.
4. Pay, S.; Baghzouz, Y. In *Effectiveness of battery-supercapacitor combination in electric vehicles*, Power Tech Conference Proceedings, 2003 IEEE Bologna, IEEE: 2003; p 6 pp. Vol. 3.
5. Wang, G.; Zhang, L.; Zhang, J., A review of electrode materials for electrochemical supercapacitors. *Chemical Society Reviews* **2012,** *41* (2), 797-828.

6. Simon, P.; Gogotsi, Y.; Dunn, B., Where do batteries end and supercapacitors begin? *Science* **2014,** *343* (6176), 1210-1211.
7. Abdelkader, A. M., Electrochemical synthesis of highly corrugated graphene sheets for high performance supercapacitors. *Journal of Materials Chemistry A* **2015,** *3* (16), 8519-8525.
8. Zhang, Y.; Li, L.; Su, H.; Huang, W.; Dong, X., Binary metal oxide: advanced energy storage materials in supercapacitors. *Journal of Materials Chemistry A* **2015,** *3* (1), 43-59.
9. Hao, P.; Tian, J.; Sang, Y.; Tuan, C.-C.; Cui, G.; Shi, X.; Wong, C.; Tang, B.; Liu, H., 1D Ni–Co oxide and sulfide nanoarray/carbon aerogel hybrid nanostructures for asymmetric supercapacitors with high energy density and excellent cycling stability. *Nanoscale* **2016,** *8* (36), 16292-16301.
10. Snook, G. A.; Kao, P.; Best, A. S., Conducting-polymer-based supercapacitor devices and electrodes. *Journal of Power Sources* **2011,** *196* (1), 1-12.
11. Wu, Z.; Zhu, Y.; Ji, X., NiCo 2 O 4-based materials for electrochemical supercapacitors. *Journal of Materials Chemistry A* **2014,** *2* (36), 14759-14772.
12. Jiang, J.; Li, Y.; Liu, J.; Huang, X.; Yuan, C.; Lou, X. W., Recent advances in metal oxide-based electrode architecture design for electrochemical energy storage. *Advanced Materials* **2012,** *24* (38), 5166-5180.
13. Aziz, A.; Zhang, T.; Lin, Y.-H.; Daneshvar, F.; Sue, H.-J.; Welland, M. E., 1D copper nanowires for flexible printable electronics and high ampacity wires. *Nanoscale* **2017,** *9* (35), 13104-13111.
14. Liu, Y.; Cao, X.; Jiang, D.; Jia, D.; Liu, J., Hierarchical CuO nanorod arrays in situ generated on three-dimensional copper foam via cyclic voltammetry oxidization for high-performance supercapacitors. *Journal of Materials Chemistry A* **2018**.
15. Xu, P.; Liu, J.; Liu, T.; Ye, K.; Cheng, K.; Yin, J.; Cao, D.; Wang, G.; Li, Q., Preparation of binder-free CuO/Cu 2 O/Cu composites: A novel electrode material for supercapacitor applications. *RSC Advances* **2016,** *6* (34), 28270-28278.
16. Chen, L.; Zhang, Y.; Zhu, P.; Zhou, F.; Zeng, W.; Lu, D. D.; Sun, R.; Wong, C., Copper salts mediated morphological transformation of Cu 2 O from cubes to hierarchical flower-like or microspheres and their supercapacitors performances. *Scientific reports* **2015,** *5*, 9672.
17. Kim, D.-W.; Rhee, K.-Y.; Park, S.-J., Synthesis of activated carbon nanotube/copper oxide composites and their electrochemical performance. *Journal of Alloys and Compounds* **2012,** *530*, 6-10.
18. Liu, Y.; Huang, H.; Peng, X., Highly enhanced capacitance of CuO nanosheets by formation of CuO/SWCNT networks through electrostatic interaction. *Electrochimica Acta* **2013,** *104*, 289-294.
19. Senthilkumar, V.; Kim, Y. S.; Chandrasekaran, S.; Rajagopalan, B.; Kim, E. J.; Chung, J. S., Comparative supercapacitance performance of CuO nanostructures for energy storage device applications. *RSC Advances* **2015,** *5* (26), 20545-20553.
20. Moosavifard, S. E.; El-Kady, M. F.; Rahmanifar, M. S.; Kaner, R. B.; Mousavi, M. F., Designing 3D highly ordered nanoporous CuO electrodes for high-performance asymmetric supercapacitors. *ACS applied materials & interfaces* **2015,** *7* (8), 4851-4860.
21. Meng, F.-L.; Zhong, H.-X.; Zhang, Q.; Liu, K.-H.; Yan, J.-M.; Jiang, Q., Integrated Cu 3 N porous nanowire array electrode for high-performance supercapacitors. *Journal of Materials Chemistry A* **2017,** *5* (36), 18972-18976.

22. Li, X.; Hao, C.; Tang, B.; Wang, Y.; Liu, M.; Wang, Y.; Zhu, Y.; Lu, C.; Tang, Z., Supercapacitor electrode materials with hierarchically structured pores from carbonization of MWCNTs and ZIF-8 composites. *Nanoscale* **2017,** *9* (6), 2178-2187.
23. Zhang, X.; Shi, W.; Zhu, J.; Kharistal, D. J.; Zhao, W.; Lalia, B. S.; Hng, H. H.; Yan, Q., High-power and high-energy-density flexible pseudocapacitor electrodes made from porous CuO nanobelts and single-walled carbon nanotubes. *ACS nano* **2011,** *5* (3), 2013-2019.
24. Zhang, W.; Yin, Z.; Chun, A.; Yoo, J.; Diao, G.; Kim, Y. S.; Piao, Y., Rose rock-shaped nano Cu2O anchored graphene for high-performance supercapacitors via solvothermal route. *Journal of Power Sources* **2016,** *318*, 66-75.
25. Dong, C.; Wang, Y.; Xu, J.; Cheng, G.; Yang, W.; Kou, T.; Zhang, Z.; Ding, Y., 3D binder-free Cu 2 O@ Cu nanoneedle arrays for high-performance asymmetric supercapacitors. *Journal of Materials Chemistry A* **2014,** *2* (43), 18229-18235.
26. Daneshvar-Fatah, F.; Wang, C.; Shaw, L. In *Synthesis of Graphene-Supported Nano-Na3MnCO3PO4 for High Rate and High Capacity Sodium Ion Batteries*, Meeting Abstracts, The Electrochemical Society: 2015; pp 12-12.
27. Lee, C. Y.; Tsai, H. M.; Chuang, H. J.; Li, S. Y.; Lin, P.; Tseng, T. Y., Characteristics and electrochemical performance of supercapacitors with manganese oxide-carbon nanotube nanocomposite electrodes. *Journal of the Electrochemical Society* **2005,** *152* (4), A716-A720.
28. Fisher, R. A.; Watt, M. R.; Ready, W. J., Functionalized carbon nanotube supercapacitor electrodes: a review on pseudocapacitive materials. *ECS Journal of Solid State Science and Technology* **2013,** *2* (10), M3170-M3177.
29. Wang, K.; Zhao, C.; Min, S.; Qian, X., Facile synthesis of Cu2O/RGO/Ni (OH) 2 nanocomposite and its double synergistic effect on supercapacitor performance. *Electrochimica Acta* **2015,** *165*, 314-322.
30. Zhi, M.; Xiang, C.; Li, J.; Li, M.; Wu, N., Nanostructured carbon–metal oxide composite electrodes for supercapacitors: a review. *Nanoscale* **2013,** *5* (1), 72-88.
31. Sugimoto, W.; Shibutani, T.; Murakami, Y.; Takasu, Y., Charge Storage Capabilities of Rutile-Type RuO2 VO 2 Solid Solution for Electrochemical Supercapacitors. *Electrochemical and solid-state letters* **2002,** *5* (7), A170-A172.
32. Jayalakshmi, M.; Rao, M. M.; Venugopal, N.; Kim, K.-B., Hydrothermal synthesis of SnO2–V2O5 mixed oxide and electrochemical screening of carbon nano-tubes (CNT), V2O5, V2O5–CNT, and SnO2–V2O5–CNT electrodes for supercapacitor applications. *Journal of Power Sources* **2007,** *166* (2), 578-583.
33. Shakir, I.; Ali, Z.; Bae, J.; Park, J.; Kang, D. J., Layer by layer assembly of ultrathin V 2 O 5 anchored MWCNTs and graphene on textile fabrics for fabrication of high energy density flexible supercapacitor electrodes. *Nanoscale* **2014,** *6* (8), 4125-4130.
34. Ramani, M.; Haran, B. S.; White, R. E.; Popov, B. N.; Arsov, L., Studies on activated carbon capacitor materials loaded with different amounts of ruthenium oxide. *Journal of Power Sources* **2001,** *93* (1-2), 209-214.
35. Sun, D.; Everett, W. N.; Chu, C. C.; Sue, H. J., Single-Walled Carbon-Nanotube Dispersion with Electrostatically Tethered Nanoplatelets. *Small* **2009,** *5* (23), 2692-2697.
36. Daneshvar-Fatah, F.; Nasirpouri, F., A study on electrodeposition of Ni-noncovalnetly treated carbon nanotubes nanocomposite coatings with desirable mechanical and anti-corrosion properties. *Surface and Coatings Technology* **2014,** *248*, 63-73.

37. Okpalugo, T. I. T.; Papakonstantinou, P.; Murphy, H.; McLaughlin, J.; Brown, N. M. D., High resolution XPS characterization of chemical functionalised MWCNTs and SWCNTs. *Carbon* **2005,** *43* (1), 153-161.
38. Kundu, S.; Wang, Y.; Xia, W.; Muhler, M., Thermal stability and reducibility of oxygen-containing functional groups on multiwalled carbon nanotube surfaces: A quantitative high-resolution xps and TPD/TPR study. *Journal of Physical Chemistry C* **2008,** *112* (43), 16869-16878.
39. Abdelkader, A.; Kinloch, I.; Dryfe, R., High-yield electro-oxidative preparation of graphene oxide. *Chemical Communications* **2014,** *50* (61), 8402-8404.
40. Pan, H.; Poh, C. K.; Feng, Y. P.; Lin, J., Supercapacitor electrodes from tubes-in-tube carbon nanostructures. *Chemistry of Materials* **2007,** *19* (25), 6120-6125.
41. An, G.; Na, N.; Zhang, X.; Miao, Z.; Miao, S.; Ding, K.; Liu, Z., SnO2/carbon nanotube nanocomposites synthesized in supercritical fluids: highly efficient materials for use as a chemical sensor and as the anode of a lithium-ion battery. *Nanotechnology* **2007,** *18* (43), 435707.
42. Hussain, Z.; Salim, M. A.; Khan, M. A.; Khawaja, E. E., X-ray photoelectron and auger spectroscopy study of copper-sodium-germanate glasses. *Journal of Non-Crystalline Solids* **1989,** *110* (1), 44-52.
43. Baddorf, A. P.; Wendelken, J. F., High coverages of oxygen on Cu(110) investigated with XPS, LEED, and HREELS. *Surface Science* **1991,** *256* (3), 264-271.
44. Jolley, J. G.; Geesey, G. G.; Hankins, M. R.; Wright, R. B.; Wichlacz, P. L., Auger electron and X-ray photoelectron spectroscopic study of the biocorrosion of copper by alginic acid polysaccharide. *Applied Surface Science* **1989,** *37* (4), 469-480.
45. Yu, Z.; Tetard, L.; Zhai, L.; Thomas, J., Supercapacitor electrode materials: nanostructures from 0 to 3 dimensions. *Energy & Environmental Science* **2015,** *8* (3), 702-730.
46. Cetinkaya, T.; Uysal, M.; Guler, M. O.; Akbulut, H.; Alp, A., Improvement cycleability of core–shell silicon/copper composite electrodes for Li-ion batteries by using electroless deposition of copper on silicon powders. *Powder Technology* **2014,** *253*, 63-69.
47. Lang, X.; Hirata, A.; Fujita, T.; Chen, M., Nanoporous metal/oxide hybrid electrodes for electrochemical supercapacitors. *Nature nanotechnology* **2011,** *6* (4), 232.
48. Zhang, L.; Tang, C.; Gong, H., Temperature effect on the binder-free nickel copper oxide nanowires with superior supercapacitor performance. *Nanoscale* **2014,** *6* (21), 12981-12989.
49. Yu, L.; Jin, Y.; Li, L.; Ma, J.; Wang, G.; Geng, B.; Zhang, X., 3D porous gear-like copper oxide and their high electrochemical performance as supercapacitors. *CrystEngComm* **2013,** *15* (38), 7657-7662.
50. Li, Y.; Chang, S.; Liu, X.; Huang, J.; Yin, J.; Wang, G.; Cao, D., Nanostructured CuO directly grown on copper foam and their supercapacitance performance. *Electrochimica Acta* **2012,** *85*, 393-398.
51. Velmurugan, V.; Srinivasarao, U.; Ramachandran, R.; Saranya, M.; Grace, A. N., Synthesis of tin oxide/graphene (SnO2/G) nanocomposite and its electrochemical properties for supercapacitor applications. *Materials Research Bulletin* **2016,** *84*, 145-151.
52. Prasad, K. R.; Miura, N., Electrochemical synthesis and characterization of nanostructured tin oxide for electrochemical redox supercapacitors. *Electrochemistry communications* **2004,** *6* (8), 849-852.

53. Li, F.; Song, J.; Yang, H.; Gan, S.; Zhang, Q.; Han, D.; Ivaska, A.; Niu, L., One-step synthesis of graphene/SnO2 nanocomposites and its application in electrochemical supercapacitors. *Nanotechnology* **2009,** *20* (45), 455602.
54. Lim, S.; Huang, N.; Lim, H., Solvothermal synthesis of SnO2/graphene nanocomposites for supercapacitor application. *Ceramics International* **2013,** *39* (6), 6647-6655.
55. Hwang, S.-W.; Hyun, S.-H., Synthesis and characterization of tin oxide/carbon aerogel composite electrodes for electrochemical supercapacitors. *Journal of Power Sources* **2007,** *172* (1), 451-459.
56. Shinde, S. K.; Dubal, D. P.; Ghodake, G. S.; Fulari, V. J., Hierarchical 3D-flower-like CuO nanostructure on copper foil for supercapacitors. *RSC Advances* **2015,** *5* (6), 4443-4447.
57. Grugeon, S.; Laruelle, S.; Herrera-Urbina, R.; Dupont, L.; Poizot, P.; Tarascon, J. M., Particle Size Effects on the Electrochemical Performance of Copper Oxides toward Lithium. *Journal of the Electrochemical Society* **2001,** *148* (4), A285-A292.
58. Chen, W.; Fan, Z.; Gu, L.; Bao, X.; Wang, C., Enhanced capacitance of manganese oxide via confinement inside carbon nanotubes. *Chemical Communications* **2010,** *46* (22), 3905-3907.
59. Zhang, H.; Song, H.; Chen, X.; Zhou, J., Enhanced lithium ion storage property of Sn nanoparticles: the confinement effect of few-walled carbon nanotubes. *The Journal of Physical Chemistry C* **2012,** *116* (43), 22774-22779.
60. Chen, W.; Pan, X.; Willinger, M.-G.; Su, D. S.; Bao, X., Facile autoreduction of iron oxide/carbon nanotube encapsulates. *Journal of the American Chemical Society* **2006,** *128* (10), 3136-3137.
61. Ng, M.-F.; Zheng, J.; Wu, P., Evaluation of Sn nanowire encapsulated carbon nanotube for a Li-ion battery anode by DFT calculations. *The Journal of Physical Chemistry C* **2010,** *114* (18), 8542-8545.
62. Yu, C.; Masarapu, C.; Rong, J.; Wei, B.; Jiang, H., Stretchable supercapacitors based on buckled single-walled carbon-nanotube macrofilms. *Advanced Materials* **2009,** *21* (47), 4793-4797.
63. Wang, G.; Huang, J.; Chen, S.; Gao, Y.; Cao, D., Preparation and supercapacitance of CuO nanosheet arrays grown on nickel foam. *Journal of Power Sources* **2011,** *196* (13), 5756-5760.
64. Hu, C.-C.; Wang, C.-C.; Chang, K.-H., A comparison study of the capacitive behavior for sol–gel-derived and co-annealed ruthenium–tin oxide composites. *Electrochimica acta* **2007,** *52* (7), 2691-2700.